

# Learning to Map for Active Semantic Goal Navigation

Georgios Georgakis<sup>\*1</sup>, Bernadette Bucher<sup>\*1</sup>, Karl Schmeckpeper<sup>1</sup>, Siddharth Singh<sup>1,2</sup>, Kostas Daniilidis<sup>1</sup>  
<sup>1</sup>University of Pennsylvania  
<sup>2</sup>Amazon

{ggeorgak, bucherb, karls}@seas.upenn.edu, hartsid@amazon.com, costas@cis.upenn.edu

## Abstract

We consider the problem of object goal navigation in unseen environments. In our view, solving this problem requires learning of contextual semantic priors, a challenging endeavour given the spatial and semantic variability of indoor environments. Current methods learn to implicitly encode these priors through goal-oriented navigation policy functions operating on spatial representations that are limited to the agent’s observable areas. In this work, we propose a novel framework that actively learns to generate semantic maps outside the field of view of the agent and leverages the uncertainty over the semantic classes in the unobserved areas to decide on long term goals. We demonstrate that through this spatial prediction strategy, we are able to learn semantic priors in scenes that can be leveraged in unknown environments. Additionally, we show how different objectives can be defined by balancing exploration with exploitation during searching for semantic targets. Our method is validated in the visually realistic environments offered by the Matterport3D dataset and show state of the art results on the object goal navigation task.

## 1. Introduction

What enables biological systems to successfully navigate to semantic targets in novel environments? Consider the example of a dog whose food tray at its own house is situated next to the fridge. Upon entering a new house for the first time, the dog will look for its food tray next to the fridge, even though the new house can largely differ in appearance and layout. This is remarkable, as it suggests that the dog is able to encode spatial associations between semantic entities that can be leveraged when trying to accomplish a navigation task. Humans exhibit the same skills in similar scenarios, albeit more nuanced, since given existing observations we can consciously choose to trust our prior knowledge over the semantic structure of the world, or to

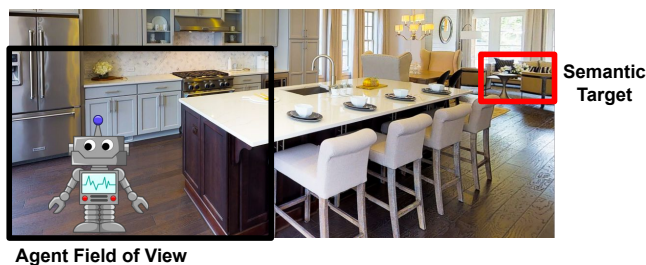


Figure 1. The navigation target of a sofa exists outside the robot’s field of view in this scene. Given contextual semantic information, the robot should not expect a sofa to be in the room with the observed refrigerator and stove, so it should select navigation goals outside of the kitchen.

continue exploring the environment. In other words, if we have a partial view of a room containing an oven, we can infer that a fridge most likely exists in the unobserved space. In addition, if we are trying to reach the sofa, then we can infer with high certainty that it will be located in a different room, as shown in the example in Figure 1. This implies that we have internal mechanisms for quantifying the uncertainty of inferred information from unobserved spaces, which guides our decision making process.

Inspired by these observations, in this work, we study the problem of object goal navigation for robotic agents in unseen environments and propose an active learning method for encoding semantic priors in indoor scenes. Our approach involves learning a mapping model that can predict (hallucinate) semantics in unobserved regions of the map containing both objects (e.g. chairs, beds) and structures (e.g. floor, wall), and during testing uses the uncertainty over these predictions to plan a path towards the target. Contrary to traditional approaches for mapping and navigation problems [8] (i.e. SLAM) where the focus is on building accurate 3D metric maps, our uncertainty formulation is designed to capture our lack of confidence about whether a certain object exists at a particular location. This results in a much more meaningful representation, suitable for target-driven tasks.

\* Denotes equal contribution.

Recently, learned approaches to navigation have been gaining popularity, where initial efforts in addressing target-driven navigation focused on end-to-end reactive approaches that learn to map pixels directly to actions [58, 37]. These methods do not have an explicit representation of the environment and tend to suffer from poor generalization. To remedy this issue, most current methods learn a map representation that enables the encoding of prior information about the geometry and semantics of a scene, acting as an episodic memory [12, 11, 25, 23]. However, maps created by these methods are restricted to contain information only from areas that the agent has directly observed. Moreover, the semantic priors are usually encoded implicitly by goal oriented navigation policy functions [14] and are, thus, target-dependent. More relevant to ours, other works have introduced spatial prediction models that either anticipate occupancy [42] or room layouts [38] beyond the agent’s field of view and demonstrated improved performance on navigation tasks. Our work differs from these methods in three principled ways: 1) We formulate an active training strategy for learning the semantic maps, 2) we exploit the uncertainty over the predictions in the planning process, and 3) while occupancy anticipation mainly learns to extend what it already sees, applying the same concept to semantics is not trivial. The latter needs to learn semantic patterns (e.g. tables are usually surrounded by chairs) in order to infer semantic information in unobserved regions.

To this end, we introduce *Learning to Map* (L2M), a novel framework for object-goal navigation consisting of two parts. First, we actively learn an ensemble of hierarchical segmentation models by choosing training samples through an information gain objective. The models operate on top-down maps and predict both occupancy and semantic regions. Second, we estimate the model uncertainty through the disagreement [41] of ensemble models, and show its effectiveness in defining objectives in planners to actively select long-term goals for semantic navigation. In addition, during test time navigation, our use of model uncertainty balances exploration with exploitation to improve performance in finding semantic targets. Our contributions are three-fold: 1) We propose a novel framework for learning to predict unobserved areas of occupancy and semantic maps, 2) We introduce uncertainty-based objectives both for actively learning to map and for selecting long-term goals during testing and provide evaluations over these different objectives, 3) We show state of the art results on the object navigation task in Matterport3D [10] dataset using the Habitat [45] simulator.

## 2. Related Work

**Semantic SLAM.** Classical approaches for navigation build large-scale 3D point cloud representations of the environment, which were required to support tasks such as

localization and path planning [8]. While these methods are typically purely geometric, several SLAM methods have attempted to associate semantic information to the reconstructed geometric map, mainly at the object-level [44, 54, 35, 6, 33]. For example, in [35] instance segmentations predicted by Mask R-CNN [26] are incorporated to facilitate per-object reconstructions, while the work of [6] proposes a probabilistic formulation to address uncertain object data association. However, SLAM systems rarely consider active exploration as they are not naturally compatible with task-driven learnable representations from deep learning architectures that can encode semantic information. Other recent works [30, 9] have sought to build 2D semantic maps and focused either on semantic transfer of a global scene in the absence of a navigation task [30], or assumed the environments were accessible before-hand [9]. In contrast, our proposed approach tackles the object goal task in unknown environments by actively learning how to predict semantics in both observed and unobserved areas of the map around the agent.

**Learning based navigation methods.** There has been a recent surge of learning based methods [58, 37, 50, 25, 17, 12, 23, 11, 19] for indoor navigation tasks [2, 5, 18, 49, 15, 51], propelled by the introduction of high quality simulators [52, 45, 32] and visually realistic environments [52, 10]. Methods which use explicit task-dependent map representations [39, 25, 12, 11, 23, 24, 28, 36] have shown to generalize better in unknown environments than end-to-end approaches with implicit world representations. For example, in [25] a differentiable mapper learns to predict top-down egocentric views of the scene from RGB images, which are then passed to a differentiable planner that predicts actions. The work of [12] presents a modular architecture that learns to build occupancy maps for the exploration task, while in [11] Mask R-CNN is used to build a top-down semantic map of the scene, followed by a learned policy that predicts goal locations in the map. More conceptually similar to our method, are approaches that attempt to encode semantic priors when learning a navigation policy. [55] uses Graph Convolutional Networks to incorporate prior semantic knowledge in a deep reinforcement learning framework, while [14] learns semantic associations by defining a topological map over the 2D scene. Finally, [38] learns to predict room layouts in unobserved regions of the map in an attempt to model architectural regularities in houses for the task of room navigation. In contrast to all these works we formulate an active, target-independent strategy to predict semantic maps and define goal selection objectives.

**Uncertainty Estimation.** Many recent works estimate uncertainty of deep learning models [20, 1]. We leverage the approach first proposed by [47] to estimate our model (epistemic) uncertainty with the variance between the out-

put of an ensemble of models. This was first used for active exploration in vision-based reinforcement learning by [41]. Maximizing epistemic uncertainty is used as a proxy for maximizing information gain [47, 41]. We use this uncertainty objective to actively fine-tune our models with a training procedure similar to the active learning approaches leveraged during training presented by [7, 13, 46]. In particular, [13] uses this active training method to improve performance on a semantic segmentation model, leading us to initially hypothesize analogous results would be possible for our semantic hallucination task. We also use this epistemic uncertainty estimate to construct confidence bounds for our estimated probability distribution which we use to select goals for target-driven navigation at test time. Both lower [22] and upper [3] confidence bound strategies for balancing exploration, exploitation, and safety have been previously proposed in the multi-armed bandit literature and extended for use in MDPs [4] and reinforcement learning [16].

### 3. Semantic Map Prediction

We propose to focus specifically on learning how to map by predicting the semantic information outside the field of view of the agent. We emphasize that this goes beyond traditional mapping (i.e. accumulating multiple views in an agent’s path) as it relies on prior information encoded as spatial associations between semantic entities in order to hallucinate the missing information. Motivated by the past success of semantic segmentation models in learning contextual information [57, 56], we formulate the semantic map prediction as a hierarchical segmentation problem. Our method takes as input an incomplete occupancy region  $p_t \in \mathbb{R}^{|C^o| \times h \times w}$  and a ground-projected semantic segmentation  $\hat{s}_t \in \mathbb{R}^{|C^s| \times h \times w}$  at time-step  $t$ . The output is a top-down semantic local region  $\hat{m}_t \in \mathbb{R}^{|C^s| \times h \times w}$ , where  $C^o$  is the set of occupancy classes containing *unknown*, *occupied*, and *free*,  $C^s$  is the set of semantic object classes, and  $h, w$  are the dimensions of the local crop. Both the inputs and the output can be seen in Figure 2. To obtain  $p_t$  we use the provided camera intrinsics and depth observation at time  $t$  to first get a point cloud which is then discretized and ground-projected similar to [42]. To estimate  $\hat{s}_t$  we first train a UNet [43] model to predict the semantic segmentation of the RGB observation at time  $t$ . All local regions are egocentric, i.e., the agent is in the middle of the crop looking upwards. Each spatial location in our map (cell) has dimensions  $10cm \times 10cm$ .

The proposed hierarchical segmentation model predicts the hallucinated semantic region in two stages. First, we estimate the missing values for the occupancy crop in the unobserved areas. In other words, we learn to hallucinate unseen spatial configurations based on what is already observed. Second, given predicted occupancy, we predict the

final semantic region  $\hat{m}_t$ . These steps are realized as two UNet [43] encoder-decoder models,  $f^o$  that predicts in occupancy space, and  $f^s$  that predicts in semantic space:

$$\hat{p}_t = f^o(p_t; \theta^o) \quad \hat{m}_t = f^s(\hat{p}_t \oplus \hat{s}_t; \theta^s) \quad (1)$$

where  $\hat{p}_t$  is the predicted local occupancy crop which includes unobserved regions,  $\oplus$  refers to the concatenation operation, and  $\theta^o, \theta^s$  are the randomly initialized weights of the occupancy and semantic networks respectively. The image segmentation model is trained independently and its output  $\hat{s}_t$  conditions  $f^s$  on the egocentric single-view observation of the agent. The model is trained end-to-end using pixel-wise cross-entropy losses for both occupancy and semantic prediction. We assume that ground-truth semantic information is available such that we can generate egocentric top-down occupancy and semantic examples. This combined objective incentivizes learning to predict plausible semantic regions by having the semantic loss backpropagating gradients affecting both  $f^o$  and  $f^s$ . Also, performing this procedure hierarchically enables the initial hallucination of unknown areas over a small set of classes  $C^o$ , before expanding to the more difficult task of predicting semantic object categories  $C^s$ . An overview of the semantic map predictor can be seen in Figure 2.

At each time-step, we register the local occupancy and semantic regions to global environment maps using the provided pose of the agent. Note that in practice, instead of directly using  $p_t$  as input to  $f^o$ , we use crops from the global map that are transformed back to egocentric view. This choice takes into consideration the fact that the agent can accumulate multiple observations and is more realistic in navigation scenarios.

### 4. Uncertainty as an Objective

A key component of a robotic system is its capacity to model what it does not know. This ability enables an agent to identify failure cases and make decisions about whether to trust its predictions or continue exploring. In our semantic map prediction problem, this would translate in estimating the uncertainty over the semantic predictions at each location of the map. We considered two types of uncertainty we face in modeling vision problems with deep learning: aleatoric and epistemic uncertainty [31, 20]. First, aleatoric uncertainty is the uncertainty in the system we are modeling. Suppose the true probability of a sofa being at a specific location given an observation is 30%. Consider a scenario where our target is *sofa* and our model estimates the true probability of 30% that a sofa is at the specific location. Our model would be correct regardless of whether the sofa is present at that location. This uncertainty is reflected in the probability output of our hierarchical model that contains  $f^o$  and  $f^s$ . We denote this model  $f : (p_t, \hat{s}_t; \theta) \mapsto \hat{m}_t$

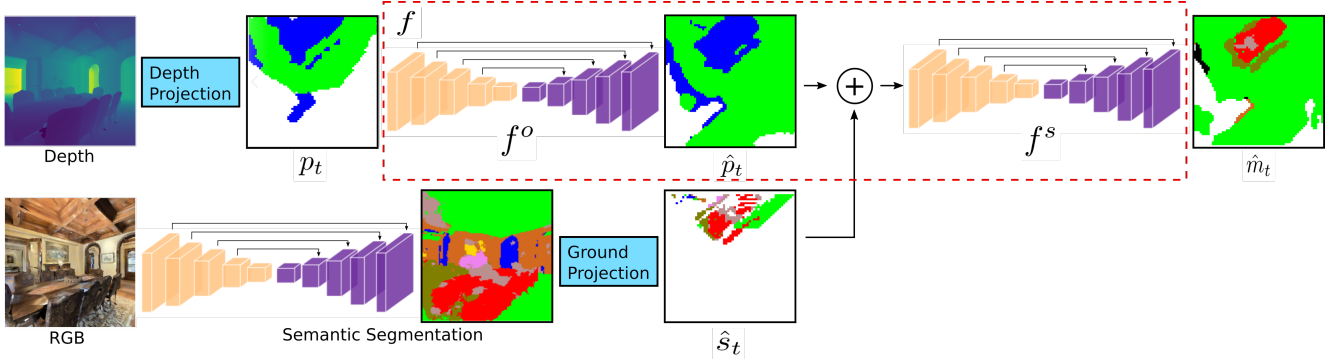


Figure 2. Overview of our semantic map predictor approach for a single time-step. The model predicts the top-down egocentric semantics of unobserved areas in a two-step procedure. First, the occupancy  $\hat{p}_t$  is predicted, which is concatenated with a ground-projected semantic segmentation of the RGB observation before producing the final output  $\hat{m}_t$ . Note that our model learns to predict semantically plausible maps (i.e. chairs surrounding a table) as shown in this example.

where  $\theta$  are the parameters of  $f$ . As shown in Figure 2,  $p_t$  is used as input to  $f$  and not  $\hat{p}_t$  which is an intermediate result.

Second, epistemic uncertainty captures the uncertainty over the model’s parameters. In training, our objective is to improve the prediction model by identifying cases it underperforms. We use epistemic uncertainty to formulate this objective, as samples with high epistemic uncertainty are associated with increased information gain. We recall that  $f$  is a classifier trained with the cross-entropy loss, so the output of  $f$  is a probability distribution. In order to estimate epistemic uncertainty, we consider the probabilistic interpretation  $P(m_t|p_t, \hat{s}_t, \theta)$  of our model  $f$  which defines a likelihood function over the parameters  $\theta$ . The parameters  $\theta$  are random variables sampled from the distribution  $q(\theta)$ . We construct  $f$  as an ensemble of hierarchical segmentation models defined over the parameters  $\{\theta_1, \dots, \theta_N\}$ . Our model estimates the true probability distribution  $P(m_t|p_t, \hat{s}_t)$  by averaging over sampled model weights,  $P(m_t|p_t, \hat{s}_t) \approx \mathbb{E}_{\theta \sim q(\theta)} f(p_t, \hat{s}_t; \theta) \approx \frac{1}{N} \sum_{i=1}^N f(p_t, \hat{s}_t; \theta_i)$  [34, 21]. Then, following prior work [47, 41], the epistemic uncertainty can be approximated from the variance between the outputs of the models in the ensemble,  $\text{Var} f(p_t, \hat{s}_t; \theta)$ .

We use uncertainty estimation in two distinct ways in our method. First, during training of the semantic predictor we actively select locations of the map with high information gain (Section 4.1). Second, during object-goal navigation we actively choose long-term goals that encourage the agent to explore in search of the target object (Section 5).

#### 4.1. Active Training

A typical procedure for training the semantic map predictor would be to sample observations along the shortest path between two randomly selected locations in a scene. However, this results in collecting a large amount of observations from repetitive or generally uninteresting areas (e.g.

spaces devoid of objects of interest). We use that naive strategy for pre-training (around 900K examples), and formulate a following step where we actively collect training samples using an information gain objective. We choose destinations for which the predictions of our pre-trained models maximize this objective. Since we can interpret our hallucinated map  $\hat{m}_t$  as a prediction  $\{\hat{s}_{t+1}, \dots, \hat{s}_{t+T}\}$  of the semantic segmentation of future observations over some window  $T$ , our greedy objective for information gain allows us to collect data in directions where we expect to make the most informative observations. The agent then moves using a local policy (described in Section 5.3). The models are then fine-tuned using the collected training examples (around 500K).

We evaluate which observations will be useful data for training by selecting  $(x, y)$ -grid locations to maximize an approximation of  $I(m_t; \theta|p_t, \hat{s}_t)$ .  $I(m_t; \theta|p_t, \hat{s}_t)$  denotes the information gain with respect to the map  $m_t$  from an update of the model parameters  $\theta$  given the occupancy observation  $p_t$  and semantic map crop  $\hat{s}_t$ . For brevity, we specify a grid location as  $l_j \in \{l_1, \dots, l_k\}$  where  $k = hw$  for an  $h \times w$  map region over which our model  $f$  estimates  $\hat{m}_t$ . We select locations which have the maximum epistemic uncertainty as a proxy for maximizing information gain [41, 47]. To this end, we define the average epistemic uncertainty across all classes. We select locations  $l_j$  from the map at time  $t$  with the greedy policy

$$\arg \max_{l_j} I(m_t; \theta|p_t, \hat{s}_t) \approx \arg \max_{l_j} \frac{1}{|C^s|} \sum_{C^s} \text{Var} f(p_t, \hat{s}_t; \theta). \quad (2)$$

In practice, these locations are selected from the accumulated uncertainty estimates in the global map. Alternatives to our chosen active training strategy include policies maximizing entropy [48] or an approximation of model infor-

mation gain using predictive entropy (BALD) [29]. We experimentally compare these alternatives to our approach in Section 6.2.

## 5. Goal Navigation Policy

We study the problem of target-driven navigation within novel environments, which can be formulated as a partially observable Markov decision process (POMDP)  $(S, A, O, P(s'|s, a), R(s, a))$ . We are interested in defining a policy that outputs goal locations as close as possible to a target class  $c$ . The state space  $S$  consists of the agent’s pose  $x$  and the semantic predictions  $\hat{m}_t$  accumulated over time in the global map. The action space  $A$  is comprised of the discrete set of locations  $h \times w$  over the map. The observation space  $O$  are the RGB-D egocentric observations, and  $P(s'|s, a)$  are the transition probabilities. A common reward choice for a supervised policy would be  $R(s, a) = D(s, c) - D(s', c)$  which is the distance reduced between the agent and the target, where  $D(\cdot, \cdot)$  is distance on the shortest path. However, this results in a target-dependent learned policy, which would require re-training when a novel target is defined. Therefore, we formulate a policy which accumulates the predicted semantic crops  $\hat{m}_t$  at every time-step, and leverages the predicted class probabilities along with uncertainty estimation over the map locations to select informative goals. An overview of our goal selection policy can be seen in Figure 3.

### 5.1. Upper Confidence Bound for Goal Selection

We now use our uncertainty-driven approach to exploration to explicitly propose an objective for goal selection. During task execution at test time,  $f$  cannot gain information because we do not update the model online with agent observations. However, the agent gains information by accumulating observations and successive predictions. We construct a policy in order to select goals from unobserved map locations using this accumulated information.

Since our task is target-driven, we can narrow our information gain objective to reduce uncertainty in areas of the map with the highest uncertainty about the target class. We denote  $f_c$  as the function  $f$  which only returns the values for a given target class  $c$ . For class  $c$ , our ensemble  $f_c$  estimates  $P_c(m_t|p_t, \hat{s}_t)$ , the probability class  $c$  is at location  $i$  given an observation  $p_t$  and semantic segmentation  $\hat{s}_t$  for each map location. The target class uncertainty at test time is given by the variance over the target class predictions  $\text{Var } f_c(p_t, \hat{s}_t; \theta)$ .

We propose selecting goals using the upper confidence bound of our estimate of  $P_c(m_t|p_t, \hat{s}_t)$  in order to select locations with high payoffs but also high potential for our model to gain new information. Upper confidence bounds have long been used to balance exploration and exploitation in problems with planning under uncertainty [3, 4, 16].

---

### Algorithm 1: L2M for ObjectNav

---

**Input:** Semantic target  $c$ ;  
Time  $t = 0$  with current position  $x_t$ ;  
Stop decision probability threshold  $S_p$ ;  
Stop decision distance threshold  $S_d$ ;  
Replan interval  $R$ ;  
**while**  $t < \text{max\_steps\_per\_episode}$  **do**  
    Observe RGB  $I_t$ , occupancy  $p_t$ ;  
    Segment  $I_t$  and ground project to compute  $\hat{s}_t$ ;  
    Hallucinate semantic map  $\hat{m}_{t,c} = \mu_c(p_t, \hat{s}_t)$ ;  
    Estimate uncertainty;  
    **if** (*Goal is reached*) **or**  
    ( $t \bmod R == 0$ ) **then**  
        | Compute Eq. 3 to select goal  $l^*$ ;  
    **end**  
    **if**  $\hat{m}_{t,c} > S_p$  at  $l_j$  on path to  $l^*$  **then**  
        | **if**  $D(x_t, l_j) < S_d$  **then**  
            | Stop decision;  
        | **end**  
    **end**  
    Navigate toward goal with DD-PPO;  
     $t = t + 1$ ;  
**end**

---

We denote  $\sigma_c(p_t, \hat{s}_t) = \sqrt{\text{Var } f_c(p_t, \hat{s}_t; \theta)}$  as the standard deviation of the target class probability, and we denote  $\mu_c(p_t, \hat{s}_t) = \frac{1}{N} \sum_{i=1}^N f_c(p_t, \hat{s}_t; \theta_i)$ . Then, we observe the upper bound  $P_c(m_t|p_t, \hat{s}_t) \leq \mu_c(p_t, \hat{s}_t) + \alpha_1 \sigma_c(p_t, \hat{s}_t)$  holds with some fixed but unknown probability where  $\alpha_1$  is a constant hyperparameter. Following [16], we use this upper bound and select goals with the policy

$$\arg \max_{l_j} (\mu_c(p_t, \hat{s}_t) + \alpha_1 \sigma_c(p_t, \hat{s}_t)). \quad (3)$$

In practice, we evaluate this objective over our map predictions and uncertainty estimations accumulated over time. Additional details of this goal selection procedure are presented in Algorithm 1.

### 5.2. Alternative Strategies

While we found our proposed upper bound strategy to choose the best candidate goal locations, we hypothesized several alternative policies which yield competitive performance. We consider the following interpretations of our uncertainty and probability estimates for object goal navigation.

- High  $\mu_c(p_t, \hat{s}_t)$ , Low  $\sigma_c(p_t, \hat{s}_t)$  : we are fairly certain we found the target object
- High  $\mu_c(p_t, \hat{s}_t)$ , High  $\sigma_c(p_t, \hat{s}_t)$  : we are uncertain we found the target object

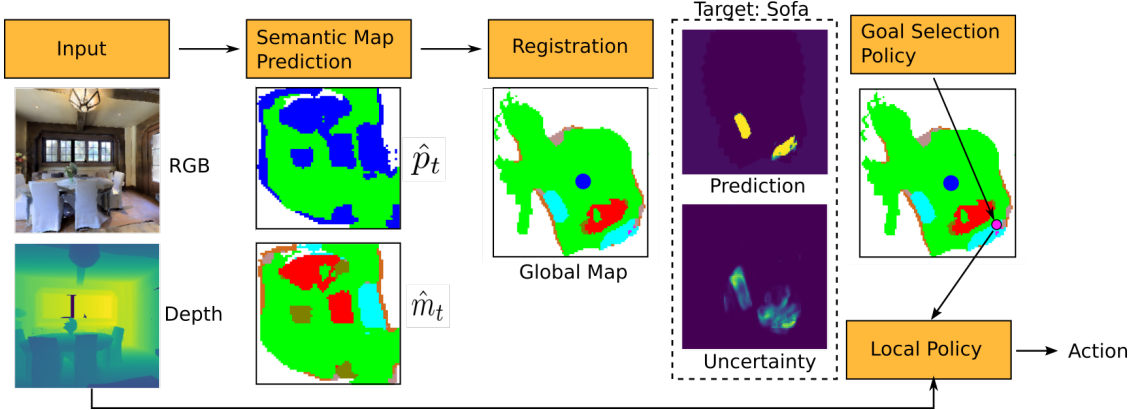


Figure 3. We select goals based on the predicted probability of a certain location containing our target and the uncertainty of the prediction at the same location. Note that in this particular example, the sofa to the right of the agent is not present in the RGB observation, but it is correctly predicted by our method.

- Low  $\mu_c(p_t, \hat{s}_t)$ , High  $\sigma_c(p_t, \hat{s}_t)$  : we are uncertain we did *not* find the target object
- Low  $\mu_c(p_t, \hat{s}_t)$ , Low  $\sigma_c(p_t, \hat{s}_t)$  : we are fairly certain we did *not* find the target object

From these interpretations we see that our upper bound strategy risks choosing locations with high potential information gain (high variance) over locations where we are fairly certain we found the target object (high probability, low variance). To consider other exploration and exploitation tradeoffs, we also observe the lower bound  $P_c(m_t|p_t, \hat{s}_t) \geq \mu_c(p_t, \hat{s}_t) - \alpha_1 \sigma_c(p_t, \hat{s}_t)$  holds with some fixed but unknown probability. Then, we can formulate the following alternative goal selection strategies.

**Lower Bound Strategy.** Lower bound strategies optimize safety [22]. We can differentiate between multiple locations which have high probability of containing our target class by choosing the one with the lowest uncertainty with the objective

$$\arg \max_{l_j} (\mu_c(p_t, \hat{s}_t) - \alpha_1 \sigma_c(p_t, \hat{s}_t)). \quad (4)$$

However, this strategy does not explore regions with high uncertainty to gain information.

**Mixed Strategy.** We can try to balance the pros and cons of the lower and upper bound strategies by switching between the two based on how high the probability is that we found the target object. We tune a hyperparameter  $\alpha_2$  to determine the cutoffs for "high" and "low" values of  $\mu_c(p_t, \hat{s}_t)$ . We select goals with the objective

$$\arg \max_{l_j} (\mu_c(p_t, \hat{s}_t) + \text{sgn}(\alpha_2 - \mu_c(p_t, \hat{s}_t)) \alpha_1 \sigma_c(p_t, \hat{s}_t)) \quad (5)$$

so that we choose a safe strategy via our lower bounds when the probability of the class at a location is high and an explo-

ration strategy via our upper bounds when the probability of the class is not high.

**Mean Strategy.** To evaluate whether our uncertainty estimate is useful, we also consider the following objective which does not incorporate uncertainty:

$$\arg \max_{l_j} \mu_c(p_t, \hat{s}_t). \quad (6)$$

### 5.3. Local Policy

Finally, in order to reach a selected goal in the map, we employ the DD-PPO [50] model that is trained with deep reinforcement learning for the task of point-goal navigation. At each time-step, this model takes as input the egocentric depth observation and the current goal converted from a 2D map coordinate to a relative distance and heading, and outputs the next navigation action for our agent.

## 6. Experiments

We perform experiments on the Matterport3D (MP3D) [10] dataset using the Habitat [45] simulator. MP3D contains reconstructions of real indoor scenes with large appearance and layout variation, and Habitat provides continuous control for realistic agent movement. We use the standard train/val split as the test set is held-out for the online Habitat challenge, which contains 56 scenes for training and 11 for validation. We conduct two key experiments.<sup>1</sup> First, we compare ablations of our method to other navigation strategies on reaching semantic targets (sec. 6.1). Second, we evaluate the performance of our semantic map predictor under different active training strategies (sec. 6.2). For all experiments we use an ensemble size  $N = 4$ .

<sup>1</sup>Additional experimental results and implementation details are presented in the appendix.

## 6.1. Object-Goal Navigation

We follow the definition of the object-goal navigation task as described in [5]. Given a semantic target (e.g. chair) the objective is to navigate to any instance of the target in the scene. Note that the agent is spawned at a random location in a novel environment for which it has no access to an existing map, nor was the map observed during the semantic map predictor training. The agent has access to RGB-D observations, gps, and compass provided by the simulator without noise. The action space consists of MOVE\_FORWARD by 25cm, TURN\_LEFT and TURN\_RIGHT by 10° and STOP. An episode is successful if the agent decides to select the STOP action while within a certain distance (1m) from the target. The agent is given a specific time-step budget to complete an episode (500 steps).

For our experiments we chose a representative set of 6 object goal categories present in MP3D: *chair, sofa, bed, cushion, counter, table*, and generated 2120 test episodes across the validation scenes. To evaluate all methods we report the following metrics: (1) **Success**: percentage of successful episodes, (2) **SPL**: Introduced in [5], this is success weighted by path length, (3) **Soft SPL**: Unlike SPL which is 0 for failed episodes, this metric is distance covered towards the goal weighted by path length. (4) **DTS**: geodesic distance of agent to the goal at the end of the episode.

**L2M Variations.** We evaluate four variations of our method with regards to the long-term goal selection and training strategies. *L2M-Active-UpperBound* refers to our proposed method that uses the semantic map predictor after active training (Section 4.1) and Eq. 3 for goal selection. *L2M-Offline-* variants use the map predictor before active training with *LowerBound*, *Mixed*, and *Mean* using Eq. 4, 5, and 6 respectively with  $\alpha_1 = 0.1$  and  $\alpha_2 = 0.75$ .

**Baselines.** Our method is compared against three competitive baselines. *L2M-Offline-FBE* [53] uses a frontier based exploration method to select long-term goals and has access to our map predictor to facilitate the stop decision. *Segm+ANS* [12]+*OracleStop* combines the exploration policy of [12] with image semantic segmentation. Since this baseline does not have access to a semantic map, it uses an oracle for the stop decision. Finally, we compare against the state-of-the-art method of *SemExp* [11] which was the winner of the CVPR 2020 Habitat ObjectNav Challenge. Since this method relies on Mask R-CNN, we evaluate on the overlapping set of categories *chair, sofa, and bed*. To facilitate a fair comparison, we use the same map resolution between our method and [11].

**Results.** Our results are presented in Table 1 showing mean and standard error performance over episodes for each of our performance metrics, while a qualitative navigation example is shown in Figure 4. We observe that our *L2M-Active-UpperBound* method outperformed all

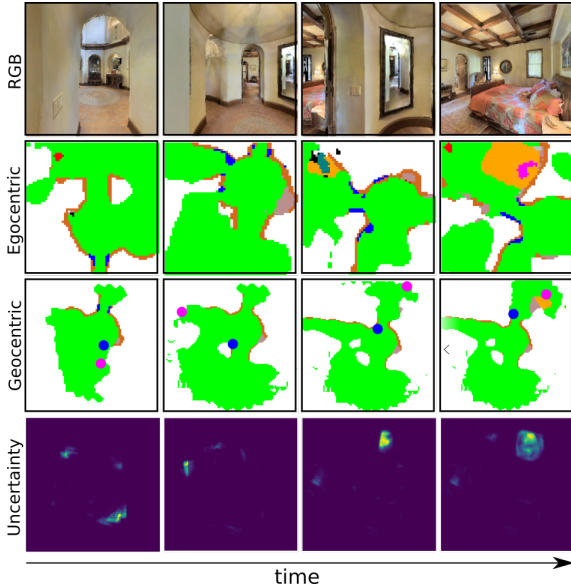


Figure 4. A navigation episode where the target object is “bed”. The agent is initially surrounded by corridors which offer limited semantic context, and is guided by the uncertainty in order to explore. In the third row, the agent is shown as a blue dot, and the selected goal as magenta.

baselines in terms of success rate by a significant margin and is comparable to *SemExp* in terms of SPL. This result is not surprising since our upper bound strategy is designed to explore and thus generally might take more steps to reach the goal. Interestingly, *L2M-Offline-FBE* outperforms *Segm.+ANS+OracleStop* even though the latter has access to the stop oracle (which results in a high SPL performance). This demonstrates the advantage of having access to our map prediction module for the object-goal navigation task. Furthermore, any performance gains of our method towards *L2M-Offline-FBE* are a direct result of our goal selection strategies. Regarding our L2M variations, we found the upper bound strategy to perform best across all metrics. We note that we expect the mixed and upper bound strategies to have close performance results since by definition the mixed strategy executes the upper bound strategy whenever the probability of the finding the target class at a given location is less than  $\alpha_2 = 0.75$ . Upper confidence bound strategies have been shown to be asymptotically optimal in simpler problems where the number of queries to a system exceeds the number of choices an agent can make [3], and empirically, we found this behavior to hold in our more complex problem scenario.

## 6.2. Active Training

We evaluate the impact of our approach to actively training our semantic mapping predictor by comparing the quality of the predicted maps generated by models trained with

Method	SPL $\uparrow$	Soft SPL $\uparrow$	Success (%) $\uparrow$	DTS (m) $\downarrow$
Random Walk	0.011 $\pm$ 0.002	0.020 $\pm$ 0.001	1.1 $\pm$ 0.2	4.846 $\pm$ 0.063
Segm. + ANS [12] + OracleStop	0.120 $\pm$ 0.006	0.126 $\pm$ 0.004	16.7 $\pm$ 0.8	4.877 $\pm$ 0.098
L2M-Offline-FBE [53]	0.055 $\pm$ 0.003	0.101 $\pm$ 0.003	21.8 $\pm$ 0.9	4.169 $\pm$ 0.079
L2M-Offline-Mean	0.096 $\pm$ 0.004	0.158 $\pm$ 0.004	31.5 $\pm$ 1.0	3.491 $\pm$ 0.08
L2M-Offline-LowerBound	0.101 $\pm$ 0.004	0.159 $\pm$ 0.004	31.6 $\pm$ 1.0	3.561 $\pm$ 0.08
L2M-Offline-Mixed	0.103 $\pm$ 0.004	0.167 $\pm$ 0.003	32.3 $\pm$ 1.0	3.442 $\pm$ 0.08
L2M-Offline-UpperBound	0.106 $\pm$ 0.004	0.168 $\pm$ 0.004	33.0 $\pm$ 1.0	3.315 $\pm$ 0.074
L2M-Active-UpperBound	<b>0.123</b> $\pm$ 0.004	<b>0.186</b> $\pm$ 0.004	<b>36.3</b> $\pm$ 1.0	<b>3.211</b> $\pm$ 0.077
SemExp* [11]	0.179 $\pm$ 0.009	-	30.1 $\pm$ 1.3	4.782 $\pm$ 0.080
L2M-Active-UpperBound*	0.170 $\pm$ 0.008	0.221 $\pm$ 0.007	39.1 $\pm$ 1.4	3.373 $\pm$ 0.119

Table 1. Comparison against baselines and variations of our method. The \* indicates that the evaluations were carried out on 3 object categories (chair, sofa, bed) instead of 6. Note that the discrepancy between the results of SemExp reported here and those in [11] are due to different sets of test episodes and object categories.

Method	IoU (%)	F1 (%)
L2M-Offline	20.1	30.5
L2M-Entropy	20.7	31.2
L2M-BALD	21.2	31.8
L2M-Active	<b>25.6</b>	<b>38.3</b>

Table 2. Comparison of active training methods in semantic map prediction.

different strategies. *L2M-Offline* is our semantic map prediction model without fine-tuning with an active strategy, while *L2M-Active* refers to the model fine-tuned with our proposed active strategy from Eq. 2. *L2M-BALD* adapts the BALD objective [29] for actively training our ensemble, and *L2M-Entropy* refers to our model fine-tuned with an entropy objective for active training [48].

We evaluate semantic prediction on the popular segmentation metrics of Intersection over Union (IoU), and F1 score. We use nine classes: *unknown*, *floor*, *wall*, plus the six semantic targets we used in the Section 6.1 experiments. We evaluate on 17900 test examples collected in the 11 validation scenes which had not been observed during training. The evaluation is conducted on predicted map crops of size  $64 \times 64$  that are collected in sequences of length 10. While the agent moves within the scene it accumulates multiple views in an occupancy map that is used as input to our method. In each crop the agent is assumed to be positioned in the middle of the crop looking upwards. The purpose of this experiment is to ascertain the quality of the predicted mapped area around the agent while it is performing a navigation task.

We observe two key results. First, Table 2 shows the overall performance of each active training method. *L2M-Active* outperforms the other methods by a significant margin. Second, we observe the per object performance on our semantic mapping results shown in Figure 4. *L2M-Active* focuses on increasing performance on challenging target

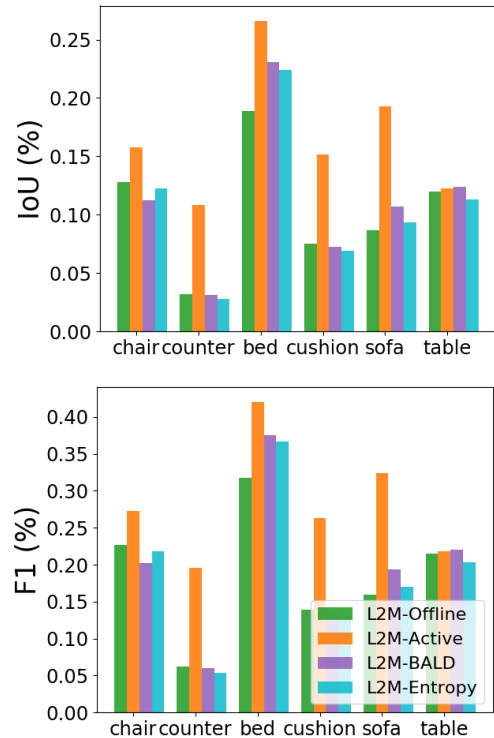


Figure 5. Semantic mapping results per class.

classes (cushion and counter) yielding more equal performance across objects in addition to higher performance overall. This behavior indicates that *L2M-Active* effectively targeted data with high epistemic uncertainty during training. Qualitative results from *L2M-Active* are presented in Figure 6.



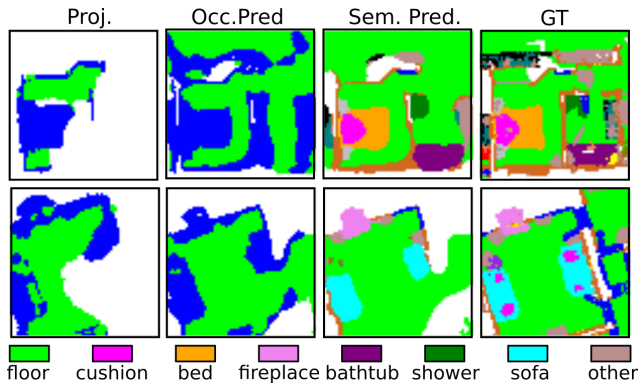


Figure 6. Qualitative map prediction results.

## 7. Conclusion

We presented *Learning to Map* (L2M), a novel framework for object-goal navigation. We hallucinate semantic map regions with an ensemble of hierarchical segmentation models. We estimate the model uncertainty through the disagreement [41] of the ensemble models, and use this uncertainty as objective to actively train our semantic map generation model. Then, we use the uncertainty estimate for a single target class to define objectives in planners to actively select long-term goals for semantic navigation. We demonstrated state of the art results on the object navigation task in Matterport3D [10] dataset using the Habitat [45] simulator.

**Limitations and Broader Impact.** Our work advances the capability of autonomous robots to navigate in novel environments which can help create a positive social impact through technologies such as robot caregivers for medically underserved populations. However, our approach has technical limitations which can yield negative social consequences. Our semantic hallucination method does not model out-of-distribution scenes and is trained on data from homes in North America and Europe. If utilized for safety critical tasks such as medical caregiving in hospitals instead of homes or in homes in different regions of the world, our method would act on biases driven by home structure in the training set with potentially harmful outcomes.

Another technical limitation of our work is our inability to model 3D relationships. We ground project 3D information from depth to a 2D map representation for occupancy, thus losing 3D spatial context. This can be important for objects such as cushions which are often on top of other objects such as sofas. Losing this context potentially contributes to our lower success rate on specific objects.

## Acknowledgments

We would like to thank Samuel Xu for implementation support in evaluating baseline methods. We are grateful for support through the Curious Minded Machines project

funded by the Honda Research Institute.

## References

- [1] Moloud Abdar, Farhad Pourpanah, Sadiq Hussain, Dana Rezazadegan, Li Liu, Mohammad Ghavamzadeh, Paul Fieguth, Xiaochun Cao, Abbas Khosravi, U Rajendra Acharya, et al. A review of uncertainty quantification in deep learning: Techniques, applications and challenges. *Information Fusion*, 2021. 2
- [2] Peter Anderson, Angel Chang, Devendra Singh Chaplot, Alexey Dosovitskiy, Saurabh Gupta, Vladlen Koltun, Jana Kosecka, Jitendra Malik, Roozbeh Mottaghi, Manolis Savva, et al. On evaluation of embodied navigation agents. *arXiv preprint arXiv:1807.06757*, 2018. 2, 13
- [3] Peter Auer, Nicolo Cesa-Bianchi, and Paul Fischer. Finite-time analysis of the multiarmed bandit problem. *Machine learning*, 47(2):235–256, 2002. 3, 5, 7
- [4] Mohammad Gheshlaghi Azar, Ian Osband, and Rémi Munos. Minimax regret bounds for reinforcement learning. In *International Conference on Machine Learning*, pages 263–272. PMLR, 2017. 3, 5
- [5] Dhruv Batra, Aaron Gokaslan, Aniruddha Kembhavi, Oleksandr Maksymets, Roozbeh Mottaghi, Manolis Savva, Alexander Toshev, and Erik Wijmans. Objectnav revisited: On evaluation of embodied agents navigating to objects. *arXiv preprint arXiv:2006.13171*, 2020. 2, 7
- [6] Sean L Bowman, Nikolay Atanasov, Kostas Daniilidis, and George J Pappas. Probabilistic data association for semantic slam. In *2017 IEEE international conference on robotics and automation (ICRA)*, pages 1722–1729. IEEE, 2017. 2
- [7] Bernadette Bucher, Karl Schmeckpeper, Nikolai Matni, and Kostas Daniilidis. An Adversarial Objective for Scalable Exploration. *arXiv preprint arXiv:2003.06082*, 2020. 3
- [8] Cesar Cadena, Luca Carlone, Henry Carrillo, Yasir Latif, Davide Scaramuzza, José Neira, Ian Reid, and John J Leonard. Past, present, and future of simultaneous localization and mapping: Toward the robust-perception age. *IEEE Transactions on robotics*, 32(6):1309–1332, 2016. 1, 2
- [9] Vincent Cartillier, Zhile Ren, Neha Jain, Stefan Lee, Irfan Essa, and Dhruv Batra. Semantic mapnet: Building allocentric semanticmaps and representations from egocentric views. *arXiv preprint arXiv:2010.01191*, 2020. 2
- [10] Angel Chang, Angela Dai, Thomas Funkhouser, Maciej Halber, Matthias Niessner, Manolis Savva, Shuran Song, Andy Zeng, and Yinda Zhang. Matterport3d: Learning from rgb-d data in indoor environments. *arXiv preprint arXiv:1709.06158*, 2017. 2, 6, 9, 11
- [11] Devendra Singh Chaplot, Dhiraj Gandhi, Abhinav Gupta, and Ruslan Salakhutdinov. Object goal navigation using goal-oriented semantic exploration. *arXiv preprint arXiv:2007.00643*, 2020. 2, 7, 8
- [12] Devendra Singh Chaplot, Dhiraj Gandhi, Saurabh Gupta, Abhinav Gupta, and Ruslan Salakhutdinov. Learning to explore using active neural slam. *arXiv preprint arXiv:2004.05155*, 2020. 2, 7, 8

- [13] Devendra Singh Chaplot, Helen Jiang, Saurabh Gupta, and Abhinav Gupta. Semantic curiosity for active visual learning. In *ECCV*, 2020. 3
- [14] Devendra Singh Chaplot, Ruslan Salakhutdinov, Abhinav Gupta, and Saurabh Gupta. Neural topological slam for visual navigation. In *Proceedings of the IEEE/CVF Conference on Computer Vision and Pattern Recognition*, pages 12875–12884, 2020. 2
- [15] Changan Chen, Ziad Al-Halah, and Kristen Grauman. Semantic audio-visual navigation. *arXiv preprint arXiv:2012.11583*, 2020. 2
- [16] Richard Y Chen, Szymon Sidor, Pieter Abbeel, and John Schulman. UCB exploration via q-ensembles. *arXiv preprint arXiv:1706.01502*, 2017. 3, 5
- [17] Tao Chen, Saurabh Gupta, and Abhinav Gupta. Learning exploration policies for navigation. *arXiv preprint arXiv:1903.01959*, 2019. 2
- [18] Abhishek Das, Samyak Datta, Georgia Gkioxari, Stefan Lee, Devi Parikh, and Dhruv Batra. Embodied question answering. In *Proceedings of the IEEE Conference on Computer Vision and Pattern Recognition*, pages 1–10, 2018. 2
- [19] Kuan Fang, Alexander Toshev, Li Fei-Fei, and Silvio Savarese. Scene memory transformer for embodied agents in long-horizon tasks. In *Proceedings of the IEEE/CVF Conference on Computer Vision and Pattern Recognition*, pages 538–547, 2019. 2
- [20] Yarin Gal. *Uncertainty in Deep Learning*. PhD thesis, University of Cambridge, 2016. 2, 3
- [21] Yarin Gal, Riashat Islam, and Zoubin Ghahramani. Deep bayesian active learning with image data. In *International Conference on Machine Learning*, pages 1183–1192. PMLR, 2017. 4
- [22] Nicolas Galichet, Michele Sebag, and Olivier Teytaud. Exploration vs exploitation vs safety: Risk-aware multi-armed bandits. In *Asian Conference on Machine Learning*, pages 245–260. PMLR, 2013. 3, 6
- [23] Georgios Georgakis, Yimeng Li, and Jana Kosecka. Simultaneous mapping and target driven navigation. *arXiv preprint arXiv:1911.07980*, 2019. 2
- [24] Daniel Gordon, Aniruddha Kembhavi, Mohammad Rastegari, Joseph Redmon, Dieter Fox, and Ali Farhadi. Iqa: Visual question answering in interactive environments. In *Proceedings of the IEEE Conference on Computer Vision and Pattern Recognition*, pages 4089–4098, 2018. 2
- [25] Saurabh Gupta, James Davidson, Sergey Levine, Rahul Sukthankar, and Jitendra Malik. Cognitive mapping and planning for visual navigation. In *Proceedings of the IEEE Conference on Computer Vision and Pattern Recognition*, pages 2616–2625, 2017. 2
- [26] Kaiming He, Georgia Gkioxari, Piotr Dollár, and Ross Girshick. Mask r-cnn. In *Proceedings of the IEEE international conference on computer vision*, pages 2961–2969, 2017. 2
- [27] Kaiming He, Xiangyu Zhang, Shaoqing Ren, and Jian Sun. Deep residual learning for image recognition. In *Proceedings of the IEEE conference on computer vision and pattern recognition*, pages 770–778, 2016. 11
- [28] Joao F Henriques and Andrea Vedaldi. Mapnet: An allocentric spatial memory for mapping environments. In *proceedings of the IEEE Conference on Computer Vision and Pattern Recognition*, pages 8476–8484, 2018. 2
- [29] Neil Houlsby, Ferenc Huszár, Zoubin Ghahramani, and Máté Lengyel. Bayesian active learning for classification and preference learning. *arXiv preprint arXiv:1112.5745*, 2011. 5, 8, 12
- [30] Yuki Katsumata, Akira Taniguchi, Lotfi El Hafi, Yoshinobu Hagiwara, and Tadahiro Taniguchi. Spcomappan: Spatial concept formation-based semantic mapping with generative adversarial networks. In *2020 IEEE/RSJ International Conference on Intelligent Robots and Systems (IROS)*, pages 7927–7934. IEEE, 2020. 2
- [31] Alex Kendall and Yarin Gal. What uncertainties do we need in bayesian deep learning for computer vision? In *Advances in neural information processing systems*, pages 5574–5584, 2017. 3
- [32] Eric Kolve, Roozbeh Mottaghi, Winson Han, Eli VanderBilt, Luca Weihs, Alvaro Herrasti, Daniel Gordon, Yuke Zhu, Abhinav Gupta, and Ali Farhadi. Ai2-thor: An interactive 3d environment for visual ai. *arXiv preprint arXiv:1712.05474*, 2017. 2
- [33] Ioannis Kostavelis and Antonios Gasteratos. Semantic mapping for mobile robotics tasks: A survey. *Robotics and Autonomous Systems*, 66:86–103, 2015. 2
- [34] Balaji Lakshminarayanan, Alexander Pritzel, and Charles Blundell. Simple and scalable predictive uncertainty estimation using deep ensembles. *arXiv preprint arXiv:1612.01474*, 2016. 4
- [35] John McCormac, Ronald Clark, Michael Bloesch, Andrew Davison, and Stefan Leutenegger. Fusion++: Volumetric object-level slam. In *2018 International Conference on 3D Vision (3DV)*, pages 32–41. IEEE, 2018. 2
- [36] Dmytro Mishkin, Alexey Dosovitskiy, and Vladlen Koltun. Benchmarking classic and learned navigation in complex 3d environments. *arXiv preprint arXiv:1901.10915*, 2019. 2
- [37] Arsalan Mousavian, Alexander Toshev, Marek Fišer, Jana Koščeká, Ayzaan Wahid, and James Davidson. Visual representations for semantic target driven navigation. In *2019 International Conference on Robotics and Automation (ICRA)*, pages 8846–8852. IEEE, 2019. 2, 13
- [38] Medhini Narasimhan, Erik Wijmans, Xinlei Chen, Trevor Darrell, Dhruv Batra, Devi Parikh, and Amanpreet Singh. Seeing the un-scene: Learning amodal semantic maps for room navigation. *arXiv preprint arXiv:2007.09841*, 2020. 2
- [39] Emilio Parisotto and Ruslan Salakhutdinov. Neural map: Structured memory for deep reinforcement learning. *arXiv preprint arXiv:1702.08360*, 2017. 2
- [40] Adam Paszke, Sam Gross, Soumith Chintala, Gregory Chanan, Edward Yang, Zachary DeVito, Zeming Lin, Alban Desmaison, Luca Antiga, and Adam Lerer. Automatic differentiation in pytorch. 2017. 11
- [41] D. Pathak, D. Gandhi, and A. Gupta. Self-Supervised Exploration via Disagreement. *ICML*, 2019. 2, 3, 4, 9
- [42] Santhosh K Ramakrishnan, Ziad Al-Halah, and Kristen Grauman. Occupancy anticipation for efficient exploration

- and navigation. *arXiv preprint arXiv:2008.09285*, 2020. [2](#), [3](#)
- [43] Olaf Ronneberger, Philipp Fischer, and Thomas Brox. U-net: Convolutional networks for biomedical image segmentation. In *International Conference on Medical image computing and computer-assisted intervention*, pages 234–241. Springer, 2015. [3](#), [11](#)
- [44] Renato F Salas-Moreno, Richard A Newcombe, Hauke Strasdat, Paul HJ Kelly, and Andrew J Davison. Slam++: Simultaneous localisation and mapping at the level of objects. In *Proceedings of the IEEE conference on computer vision and pattern recognition*, pages 1352–1359, 2013. [2](#)
- [45] Manolis Savva, Abhishek Kadian, Oleksandr Maksymets, Yili Zhao, Erik Wijmans, Bhavana Jain, Julian Straub, Jia Liu, Vladlen Koltun, Jitendra Malik, et al. Habitat: A platform for embodied ai research. In *Proceedings of the IEEE International Conference on Computer Vision*, pages 9339–9347, 2019. [2](#), [6](#), [9](#)
- [46] Ozan Sener and Silvio Savarese. Active learning for convolutional neural networks: A core-set approach. *arXiv preprint arXiv:1708.00489*, 2017. [3](#)
- [47] H Sebastian Seung, Manfred Opper, and Haim Sompolinsky. Query by committee. In *Proceedings of the fifth annual workshop on Computational learning theory*, pages 287–294, 1992. [2](#), [3](#), [4](#)
- [48] Claude E Shannon. A mathematical theory of communication. *The Bell system technical journal*, 27(3):379–423, 1948. [4](#), [8](#), [12](#)
- [49] Saim Wani, Shivansh Patel, Unnat Jain, Angel X Chang, and Manolis Savva. Multion: Benchmarking semantic map memory using multi-object navigation. *arXiv preprint arXiv:2012.03912*, 2020. [2](#)
- [50] Erik Wijmans, Abhishek Kadian, Ari Morcos, Stefan Lee, Irfan Essa, Devi Parikh, Manolis Savva, and Dhruv Batra. Dd-ppo: Learning near-perfect pointgoal navigators from 2.5 billion frames. *arXiv*, pages arXiv–1911, 2019. [2](#), [6](#)
- [51] Yi Wu, Yuxin Wu, Georgia Gkioxari, and Yuandong Tian. Building generalizable agents with a realistic and rich 3d environment. *arXiv preprint arXiv:1801.02209*, 2018. [2](#)
- [52] Fei Xia, Amir R Zamir, Zhiyang He, Alexander Sax, Jitendra Malik, and Silvio Savarese. Gibson env: Real-world perception for embodied agents. In *Proceedings of the IEEE Conference on Computer Vision and Pattern Recognition*, pages 9068–9079, 2018. [2](#)
- [53] Brian Yamauchi. A frontier-based approach for autonomous exploration. In *Proceedings 1997 IEEE International Symposium on Computational Intelligence in Robotics and Automation CIRA'97. Towards New Computational Principles for Robotics and Automation*, pages 146–151. IEEE, 1997. [7](#), [8](#)
- [54] Shichao Yang and Sebastian Scherer. Cubeslam: Monocular 3-d object slam. *IEEE Transactions on Robotics*, 35(4):925–938, 2019. [2](#)
- [55] Wei Yang, Xiaolong Wang, Ali Farhadi, Abhinav Gupta, and Roozbeh Mottaghi. Visual semantic navigation using scene priors. *arXiv preprint arXiv:1810.06543*, 2018. [2](#)
- [56] Yuhui Yuan, Xilin Chen, and Jingdong Wang. Object-contextual representations for semantic segmentation. *arXiv preprint arXiv:1909.11065*, 2019. [3](#)
- [57] Hang Zhang, Kristin Dana, Jianping Shi, Zhongyue Zhang, Xiaoang Wang, Amrith Tyagi, and Amit Agrawal. Context encoding for semantic segmentation. In *Proceedings of the IEEE conference on Computer Vision and Pattern Recognition*, pages 7151–7160, 2018. [3](#)
- [58] Yuke Zhu, Roozbeh Mottaghi, Eric Kolve, Joseph J Lim, Abhinav Gupta, Li Fei-Fei, and Ali Farhadi. Target-driven visual navigation in indoor scenes using deep reinforcement learning. In *2017 IEEE international conference on robotics and automation (ICRA)*, pages 3357–3364. IEEE, 2017. [2](#), [13](#)

## A. Appendix

Here we provide the following additional material:

1. Implementation details.
2. Additional experimental results for semantic map prediction.
3. Object goal navigation results for the different active training strategies.
4. Evaluation of our method on easy vs hard episodes.
5. Investigation of the effect of the stop decision and local policy.
6. Additional visualizations of semantic maps and navigation examples.

### A.1. Implementation Details

All UNets [43] in our implementation are combined with a backbone ResNet18 [27] for providing initial encodings of the inputs. Each UNet has four encoder and four decoder convolutional blocks with skip connections. The models are trained in the PyTorch [40] framework with Adam optimizer and a learning rate of 0.0002. All experiments are conducted with an ensemble size  $N = 4$ . For the semantic map prediction we receive RGB and depth observations of size  $256 \times 256$  and define crop and global map dimensions as  $h = w = 64$ ,  $H = W = 384$  respectively. We use  $C^s = 27$  semantic classes that we selected from the original 40 categories of MP3D [10] We generate the ground-truth for semantic crops using the 3D point clouds of the scenes which contain semantic labels. Regarding navigation, we use a threshold of 0.75 on the prediction probabilities to determine the occurrence of the target object in the map, and a stop decision distance of  $0.5m$ . Finally, we re-select a goal every 20 steps.

We executed training and testing on our internal cluster on RTX 2080 Ti GPUs. To train our final model, our image segmentation network first trained for 24 hours. Then,

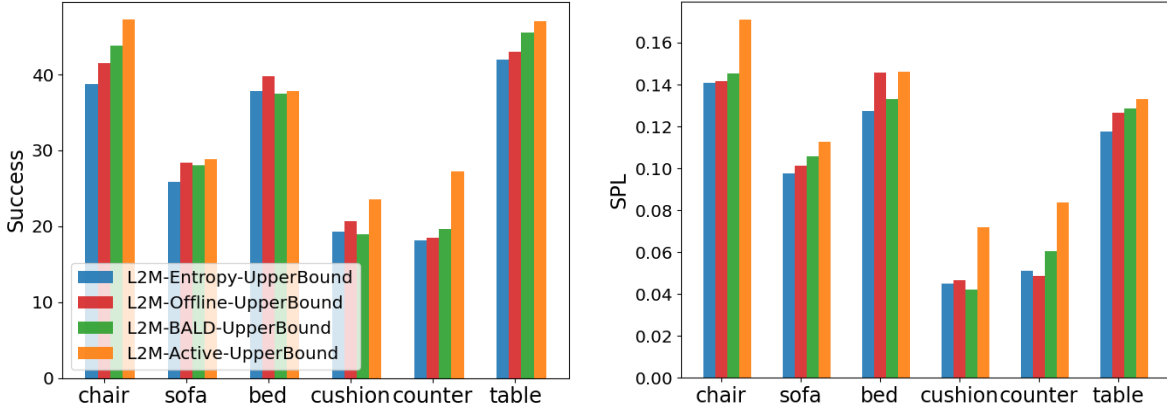


Figure 7. Navigation results per class over different active training methods.

Occupancy Prediction			
Method	Acc (%)	IoU (%)	F1 (%)
Depth Proj.	31.2	14.5	24.3
Multi-view Depth Proj.	48.5	31.0	47.0
L2M-Offline	65.2	45.5	61.9
L2M-Active	<b>68.1</b>	<b>48.8</b>	<b>65.0</b>
Semantic Prediction			
Method	Acc (%)	IoU (%)	F1 (%)
Image Segm. Proj.	13.9	5.9	10.2
Sem. Sensor Proj.	16.9	9.1	16.0
Multi-view Sem. Sensor Proj.	27.6	18.9	31.4
L2M-Offline	31.2	20.1	30.5
L2M-Active	<b>33.5</b>	<b>25.6</b>	<b>38.3</b>

Table 3. Comparison of our occupancy and semantic map predictions to non-prediction alternatives.

each model in our offline ensemble trained for 72 hours on separate GPUs. Finally, each model was fine-tuned on the actively collected data for 24 hours on separate GPUs.

## A.2. Semantic Map Prediction

Here we provide additional results for our semantic map predictor, including evaluation over occupancy predictions (*unknown, occupied, free*). The set-up for this experiment is the same as in Section 6.2 of the main paper. The purpose of this evaluation is to demonstrate the superiority of our method to possible non-prediction alternatives such as using directly the projected depth, or ground-projected image segmentation. To this end we compare against the following baselines:

- **Depth Projection:** Occupancy map estimated from a single depth observation.
- **Multi-view Depth Projection:** Occupancy map accumulated over multiple views of depth observations.
- **Image Segmentation Projection:** Our semantic segmentation model that operates on image observations,

followed by projection of resulting labels.

- **Semantic Sensor Projection:** Semantic map generated by single-view ground-truth semantic sensor images provided by the simulator.
- **Multi-view Semantic Sensor Projection:** Same as the previous baseline, but with multiple views accumulated in the semantic map.

We present mean values for accuracy, intersection over union (IoU), and F1 score in Table 3. Both our approaches outperform all baselines by a significant margin. This suggests that our predictions of unobserved areas can provide more useful information to the agent than only relying on accumulated views from egomotion. In the case of semantic prediction our results are even more compelling as they are compared against the ground-truth semantic sensor of the Habitat simulator. Note that the *Multi-view Sensor* baseline gets far from perfect score for two reasons: 1) it still contains unobserved areas, and 2) due to the pooling of the labels in the lower spatial dimensions of the top-down map (which affects all projections). In contrast, our approach is unaffected by this problem as we learn to predict semantics from depth projected inputs.

## A.3. Active Training Methods on Object Navigation

In this section we further evaluate on the object-goal navigation task the different active training strategies introduced in Section 4.1 of the main paper, while the experimental setup is identical to that of Section 6.1. Our proposed method of *L2M-Active-UpperBound* is compared to *L2M-BALD-UpperBound* and *L2M-Entropy-UpperBound* which are actively trained using predictive entropy (BALD) [29] and entropy [48] respectively. *L2M-Offline-UpperBound* uses the map predictor before active training. All methods use the strategy of Eq. 3 from the

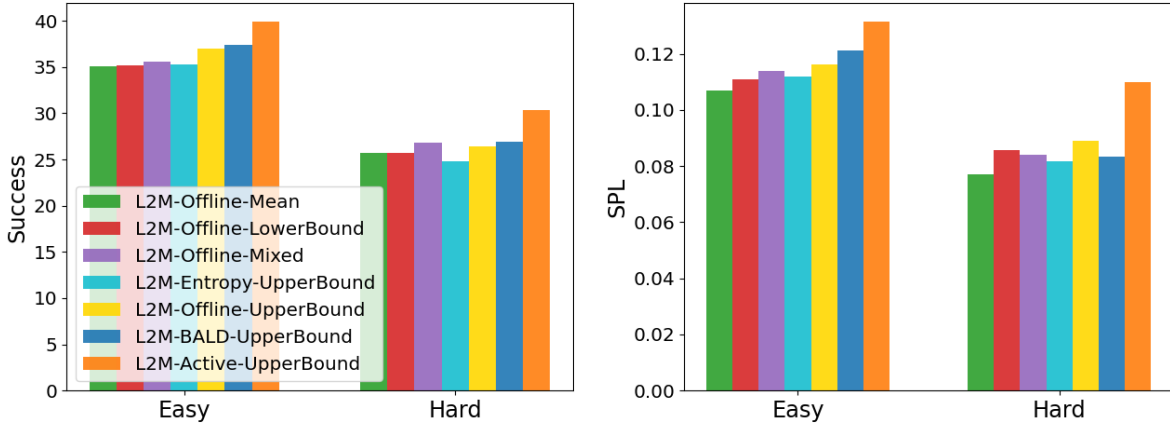


Figure 8. Our actively trained semantic mapping model seeks out difficult data during training resulting in both higher performance navigating to target objects and more consistently high performance on hard episodes.

Method	SPL $\uparrow$	Soft SPL $\uparrow$	Success (%) $\uparrow$	DTS (m) $\downarrow$
L2M-Entropy-UpperBound	0.101 $\pm$ 0.004	0.162 $\pm$ 0.004	31.3 $\pm$ 1.0	3.495 $\pm$ 0.079
L2M-Offline-UpperBound	0.106 $\pm$ 0.004	0.168 $\pm$ 0.004	33.0 $\pm$ 1.0	3.315 $\pm$ 0.074
L2M-BALD-UpperBound	0.107 $\pm$ 0.004	0.167 $\pm$ 0.004	33.4 $\pm$ 1.0	3.472 $\pm$ 0.079
L2M-Active-UpperBound	<b>0.123</b> $\pm$ 0.004	<b>0.186</b> $\pm$ 0.004	<b>36.3</b> $\pm$ 1.0	<b>3.211</b> $\pm$ 0.077

Table 4. Comparison of different active training strategies on object-goal navigation.

main paper for goal selection, which was shown to outperform other goal selection policies that we considered.

Results are shown in Table 4. Our *L2M-Active-UpperBound* outperforms its *BALD* and *Entropy* counterparts on all metrics, which validates our choice for the information gain objective presented in Section 4.1 of the main paper. Furthermore, Figure 7 presents the per-object performance of these methods. Our proposed method demonstrates higher performance increase from the other baselines on the more challenging objects (cushion and counter). This highlights that our active training successfully selected training examples with high information value.

#### A.4. Easy vs Hard Episodes

Another way of evaluating the impact of our proposed method is by analyzing its performance with respect to *easy* and *hard* episodes. We generated 1325 *easy* and 795 *hard* episodes, which combined make up our entire test set used in Section 6.1 of the main paper. The *hard* episodes are generated with larger geodesic to euclidean distance ratio between the starting position and the target (1.1 vs 1.05), which translates to more obstacles present in the path, and have larger mean geodesic distance (6.5m vs 4.5m).

Our actively trained semantic mapping model seeks out difficult data during training, resulting in more consistently high performance on both *easy* and *hard* episodes than our model when trained offline. The performance difference is

visualized in Figure 8. It is worth noting that the performance gap is higher in the case of *hard* episodes. Furthermore, regarding the comparison between the different active strategies, we observe that the results follow the same trend as in Section 6.2 of the main paper, which suggests that semantic mapping performance is correlated to success in object-goal navigation.

#### A.5. Effect of Stop Decision and Local Policy

A common source of failure in navigation tasks revolves around the stop decision, in other words, deciding to stop at the correct distance to the target in order for the episode to be considered successful. This was suggested by [2] in an attempt to make the task more realistic. Earlier end-to-end methods [58] either did not require the stop decision or had difficulties in predicting the stop action due to inherent bias of the model to other possible actions [37]. In this last experiment we investigate the impact of the stop decision in the overall success of our model by defining an oracle that provides our model with the stop decision when we are within success distance of the target. In addition, we explore the effect of the local policy by using instead shortest paths estimated by the habitat simulator.

The per-object results are shown in Figure 9. Note that these results are using the *hard* episodes as described in Section A.4. *Ours* corresponds to our proposed method of *L2M-Active-UpperBound*. For the

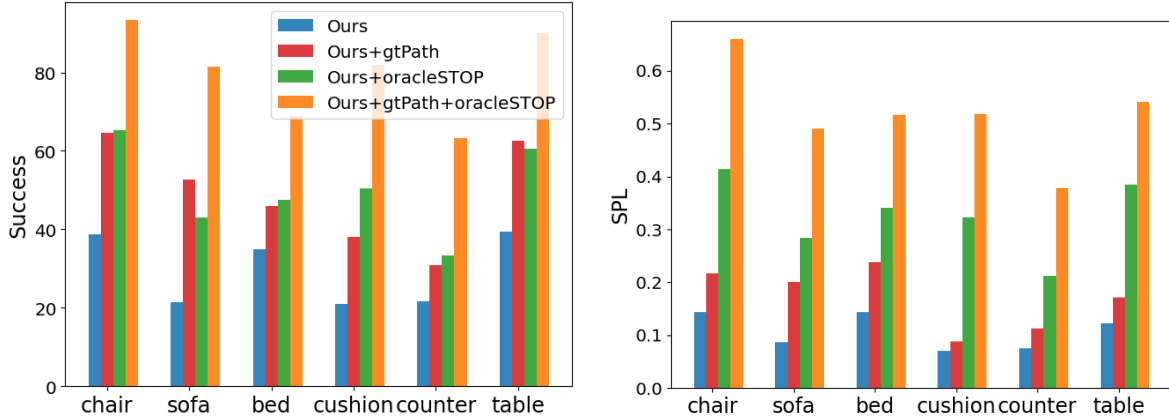


Figure 9. Ablations of our method that investigate the effect of the stop decision and local policy.

rest of the baselines we either replace the stop decision with an oracle *Ours+oracleSTOP*, use ground-truth paths instead of the local policy *Ours+gtPath*, or both *Ours+gtPath+oracleSTOP*. We observe a significant increase of performance for all baselines. In the case of *Ours+gtPath* the performance gap suggests that the local policy has difficulties reaching the goals, while in the case of *Ours+oracleSTOP* it suggests that our model selects well positioned goals but our stop decision criteria fail to recognize a goal state. Finally, *Ours+gtPath+oracleSTOP* achieves mean success rates over 80% for some objects, thus advising further investigation of these components of our pipeline.

### A.6. Additional visualizations

Finally, we provide some additional visualizations. An example navigation episode is shown in Figure 10. A set of predicted occupancy maps and corresponding semantic predictions are shown in Figure 11, while Figure 12 showcases predictions from the individual models in the ensemble.

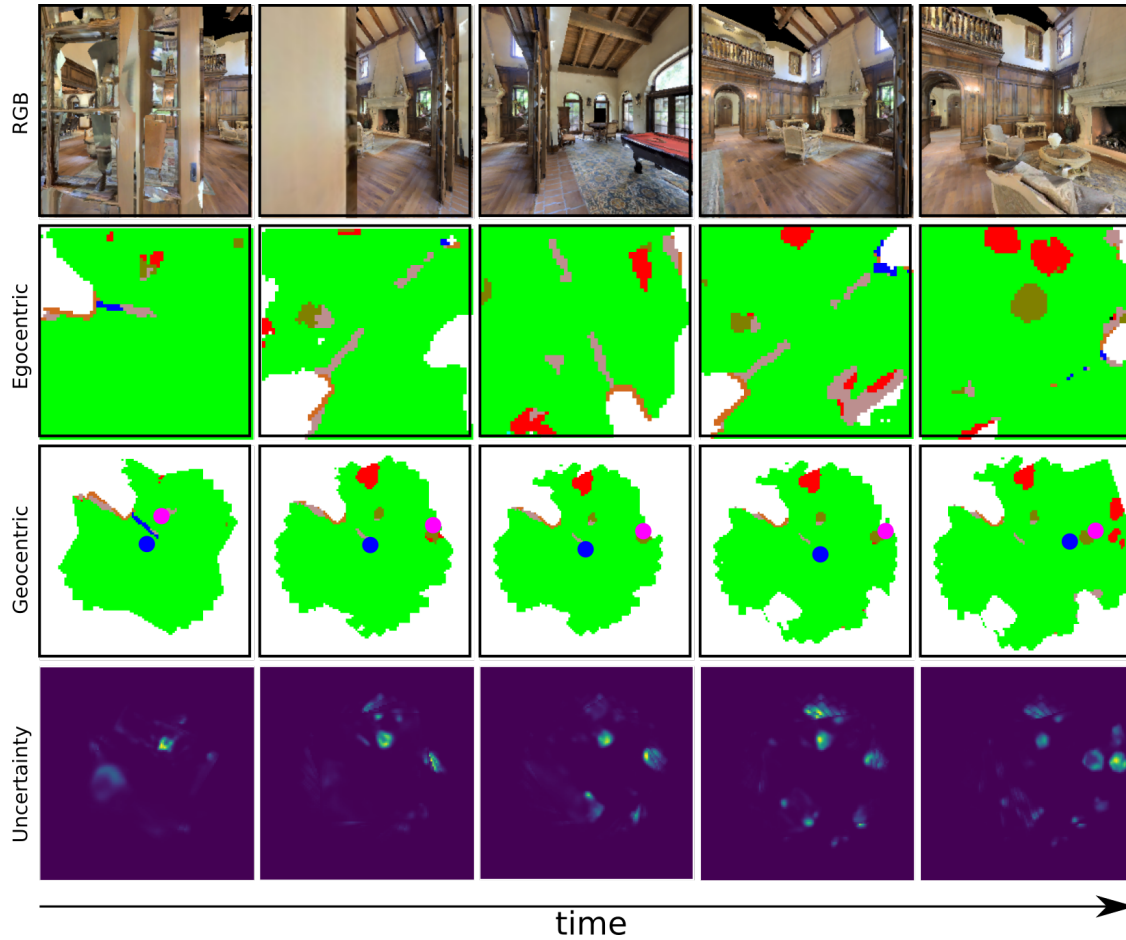


Figure 10. An example of a navigation episode where the target object is “chair”. In the third row, the agent is shown as a blue dot, and the selected goal as magenta.

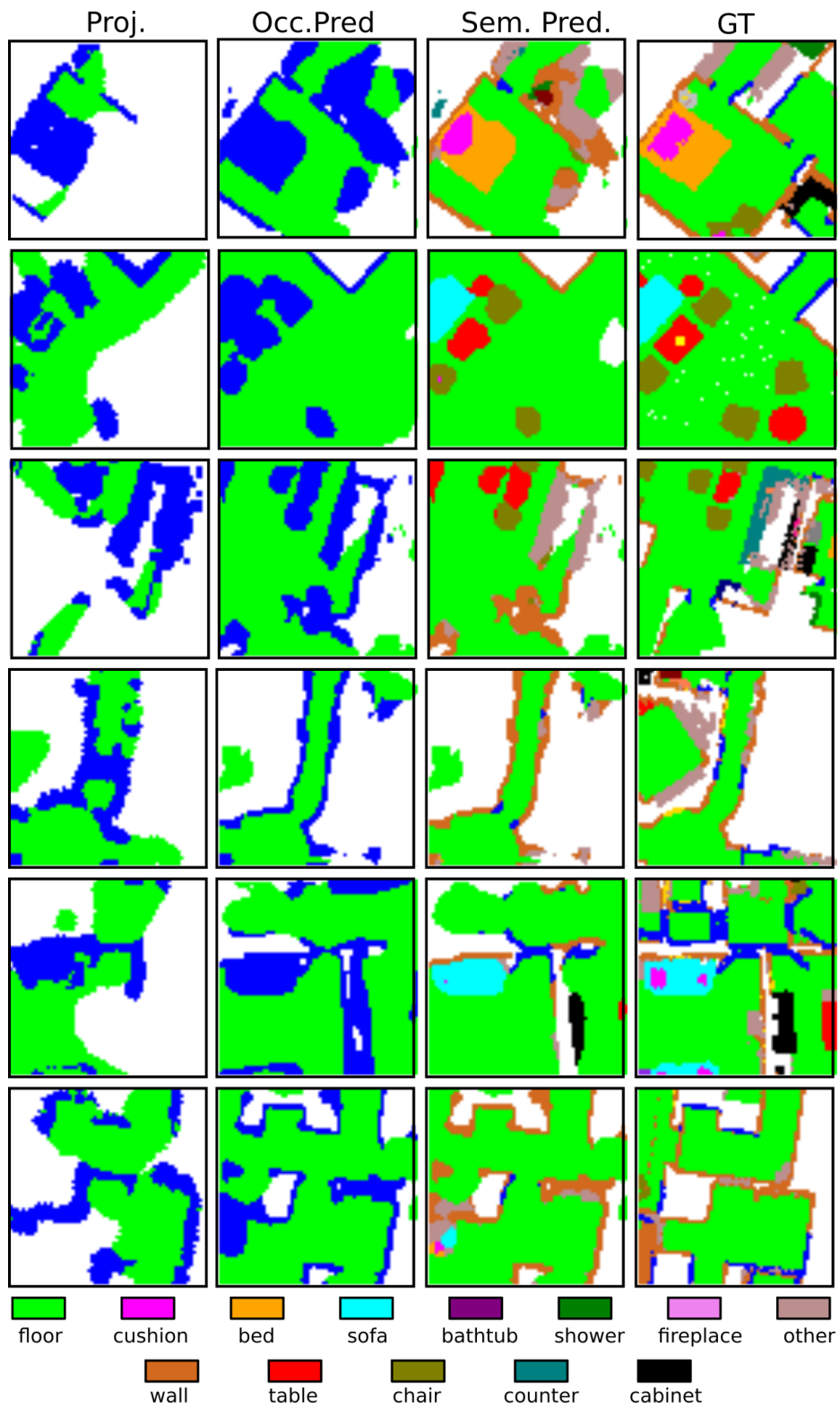


Figure 11. Qualitative occupancy and semantic prediction results using our *L2M-Active* approach.



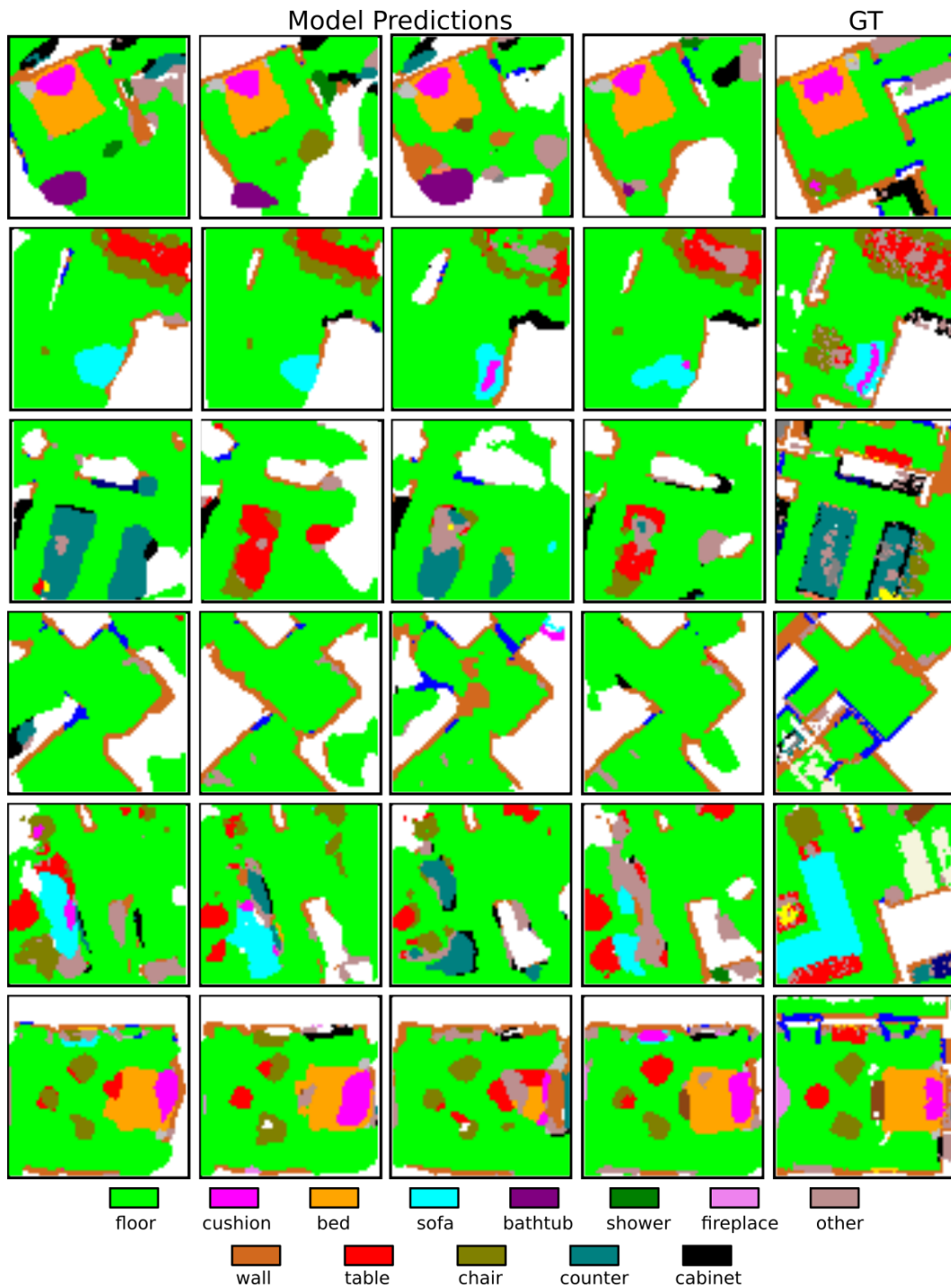


Figure 12. Qualitative semantic prediction from the individual models in the ensemble (first four columns) using our *L2M-Active* approach.